Supplementary Information to the publication in *Inorganic Chemistry* **2018:**

The magnetic structure of $SmCo_5$ from 5 K to the Curie temperature

Holger Kohlmann,*[a] Thomas C. Hansen,[b] and Vivian Nassif[b]

[a] Institute of Inorganic Chemistry, Leipzig University, Johannisallee 29, 04103 Leipzig, Germany

[b] Institut Laue-Langevin, 71 Avenue des Martyrs, CS 20156, 38042 Grenoble cedex 9, France

* Correspondence author: holger.kohlmann@uni-leipzig.de

1 Synthesis

Isotopically enriched samarium oxide powder from TRACE Sciences International (Wilmington, Delaware, USA) was used for the preparation of $^{154}Sm_2O_3$. The isotopic compositions according to the supplier (98.9(1)% ^{154}Sm, 0.8% ^{152}Sm, all others < 0.1%; chemical impurities – 630 ppm Pr, 630 ppm Gd, 500 ppm Eu, all others < 100 ppm) were confirmed by ICP-MS analysis [1]. In order to remove samarium hydroxide, $Sm(OH)_3$, the powder was annealed at 1273 K for 120 h prior to use. $^{154}Sm_2O_3$ (0.9 g) was mixed and ground with stoichiometric amounts of cobalt powder (99.8%, 1.6 µm, Alfa Aesar) under inert atmosphere in an argon filled glovebox before calcium granules (redistilled, 16 mesh, 99.5%, Alfa Aesar) were added (39% excess with respect to $^{154}Sm_2O_3$ + 10 Co + 3 Ca = 2 $^{154}SmCo_5$ + 3CaO [2]). The reaction mixture was put into a niobium ampoule, which was welded under 50 kPa argon gas and placed inside a quartz tube under dynamic vacuum (10 Pa). The temperature program for the modified ORD (oxides-reduction-diffusion) method was optimized before for $SmCo_5$ [2] and consists of heating by 200K/h to 1123 K, to 1223 K and finally to 1423 K with holding times of 1 h, 1 h, and 6 h, respectively. After cooling down with the natural rate of the furnace and opening of the niobium tube, a light grey, hard solid was obtained that could be ground to a fine powder. It was washed with 100 mL of 0.1 molar acetic acid for 5 min while continuously stirring and subsequent decanting and rinsing with deionized water. This procedure was repeated with 50 mL of 0.1 molar acetic acid until the washing liquid became colored, at which point the liquid was quickly decanted and the powder rinsed multiple times with water. Drying at 353 K yielded a dark brown material with few white particles of calcium oxide. The sample was thus finely ground and the procedure was repeated until the powder was single phase according to optical inspection and X-ray powder diffraction.

2 X-ray powder diffraction (XPD)

Laboratory XPD data were collected using flat reflection samples T = 296(1) K at a Seifert XRD3000 diffractometer with CoK_α radiation. Rietveld refinements of crystal structures were performed with the program TOPAS [3] and FullProf [4, 5].

3 Neutron powder diffraction (NPD)

2.3 g $^{154}SmCo_5$ powder was placed inside a thin-walled vanadium cylinder of 5 mm outer diameter. Neutron powder diffraction data were recorded at the high intensity two-axis powder diffractometer D1B of the Institut Laue-Langevin (ILL) in Grenoble, France. The wavelength of the diffractometer was determined to be λ = 2.5218(3) Å from refinement of the sample at T = 297(1) K with fixed lattice parameters (set to values determined before from XPD analysis (see chapter 2)). Data collection times were 5 min per pattern. First, the sample was cooled inside an orange cryostat to T = 5 K, were data collection started. The sample was then heated to 320 K with 4 K/min while continuously collecting NPD data. Heating took place subsequently in a furnace on the diffractometer D1B (1 K per 72 s up to 600 K, holding for 30 minutes, 1 K per 36 s up to 1100 K, holding for 30 minutes). Afterwards, the procedure was reversed for cooling, which had to be stopped at 531 K. Rietveld refinements of crystal structures were performed with the program FullProf [4, 5] sequentially for all investigated temperatures (Figs. S1-S14 and Tabs. S1 and S2). Structural and magnetic phases were fully constrained for crystallographic, global (zero shift, background polynomial of fourth order) and profile parameters (pseudo-Voigt function mixing parameter η, asymmetry parameter, Caglioti reflection width parameters u, v and w).

In order to check for possible diffraction contributions of the furnace, measurements without sample were also taken, revealing a small reflection around 2θ = 75°. Upon heating, its intensity increased and its position shifted towards lower angles (Figs. S1-S5). Therefore, we attribute this reflection to diffraction of the neutron beam on the heating elements or the shielding inside the furnace. Even at high temperatures, this parasitic reflection is small compared to the diffraction from the sample. Nevertheless, the quality of the Rietveld refinement is somewhat lower for high temperature data as seen by the higher residual values (Figs. S12-S14). Exclusion of the affected 2θ range was not performed due to the closeness of the main reflection of $SmCo_5$.

4 Results

Crystal and magnetic structures of $^{154}SmCo_5$ were determined by sequential Rietveld refinement on 459 neutron powder diffraction data sets. Rietveld plots showing observed, calculated and difference diagrams are shown in Fig. 1 (main manuscript, T = 5 K) and Figs. S1-S5 (selected temperatures). Graphical representations of refinement results in figures S6-S14 show blue symbols for data taken on the $^{154}SmCo_5$ sample in the cryostat, black symbols for data taken on the $^{154}SmCo_5$ sample in the furnace up to 600 K (fast heating) and red symbols for data taken on the $^{154}SmCo_5$ sample in the furnace up to 1100 K (slow heating).

Neutron powder diffraction patterns for 300 K ≤ T ≤ 320 K were taken both in the cryostat and in the furnace. The refinement results differ slightly for parameters depending on reflection position such as lattice parameters and unit cell volume (Figs. S6-S8). They are insignificant for parameters depending on intensity such as thermal displacement parameters and magnetic moments (Figs. S9-S11, Fig. 3 in the main manuscript). Therefore, we assume a small misalignment in sample position in the furnace to be causing this effect. Refinement of sample position in FullProf [4, 5] did not result in a satisfactory solution for this problem. Magnetic moments, which are in the focus of this study, are not affected by this misalignment and are therefore considered completely reliable nonetheless.

The data set recorded at 1037 K (last entry in Tab. S2), i. e. very close to the Curie temperature, did not yield a satisfactory Rietveld refinement. Results of this Rietveld refinement are included in Tab. S2 and Figs. S6-S14 for reasons of completeness. Because of its questionable validity, those data are excluded from the discussion in the main manuscript and Fig. 3.

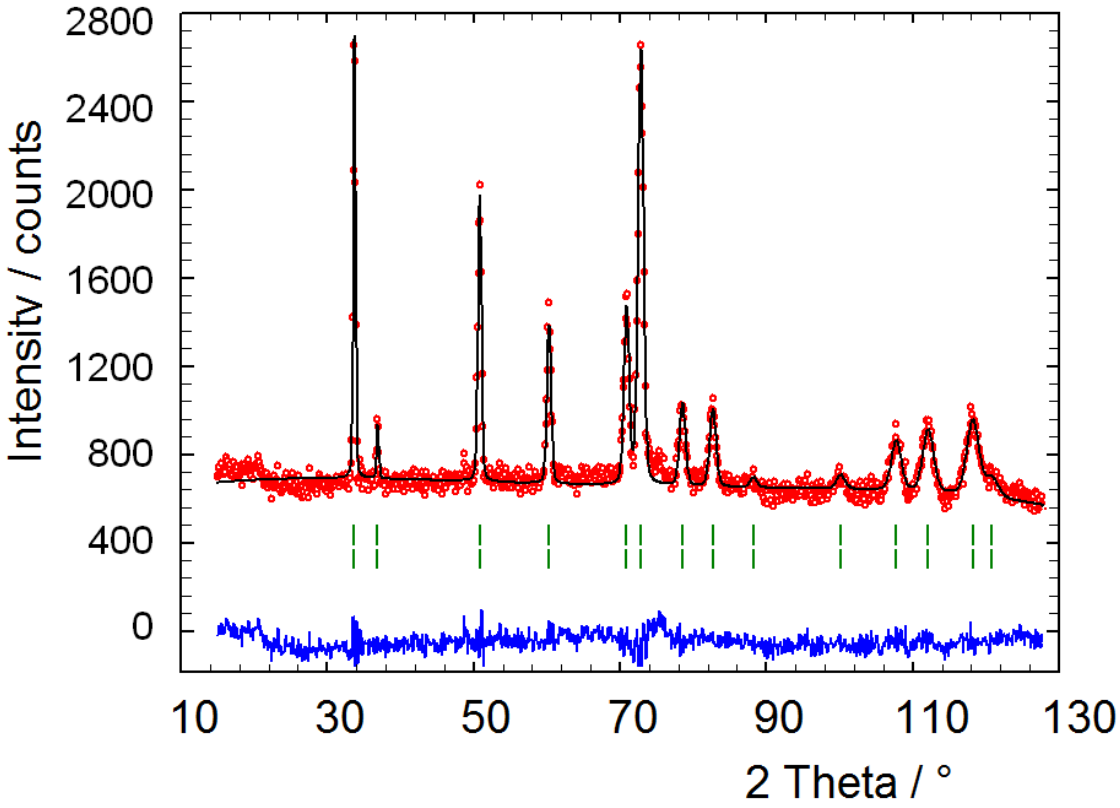

Figure S1: Rietveld refinement of the nuclear and magnetic structure of $^{154}SmCo_5$ based on neutron powder diffraction data (D1B, λ = 2.5218(3) Å, T = 300 K); from top to bottom: measured (black) and calculated (red) diffraction pattern, Bragg markers of structural and magnetic phase, difference diffraction pattern (blue).

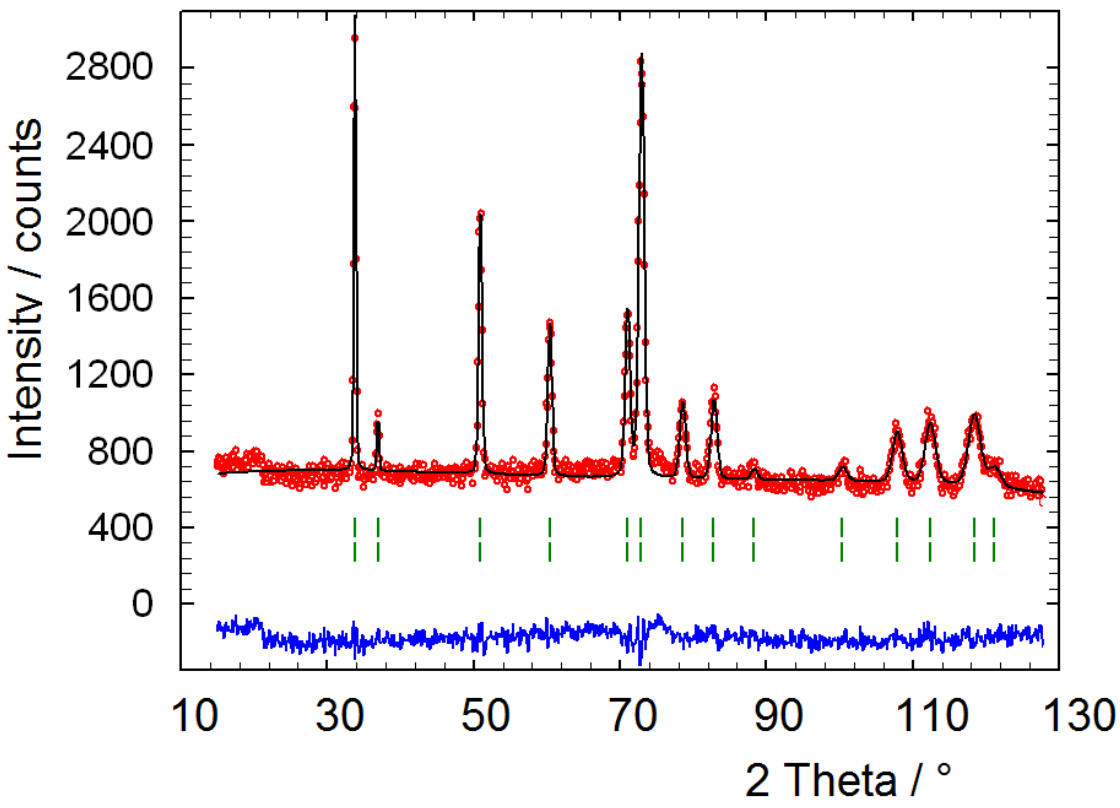

Figure S2: Rietveld refinement of the nuclear and magnetic structure of $^{154}SmCo_5$ based on neutron powder diffraction data (D1B, λ = 2.5218(3) Å, T = 503 K); from top to bottom: measured (black) and calculated (red) diffraction pattern, Bragg markers of structural and magnetic phase, difference diffraction pattern (blue).

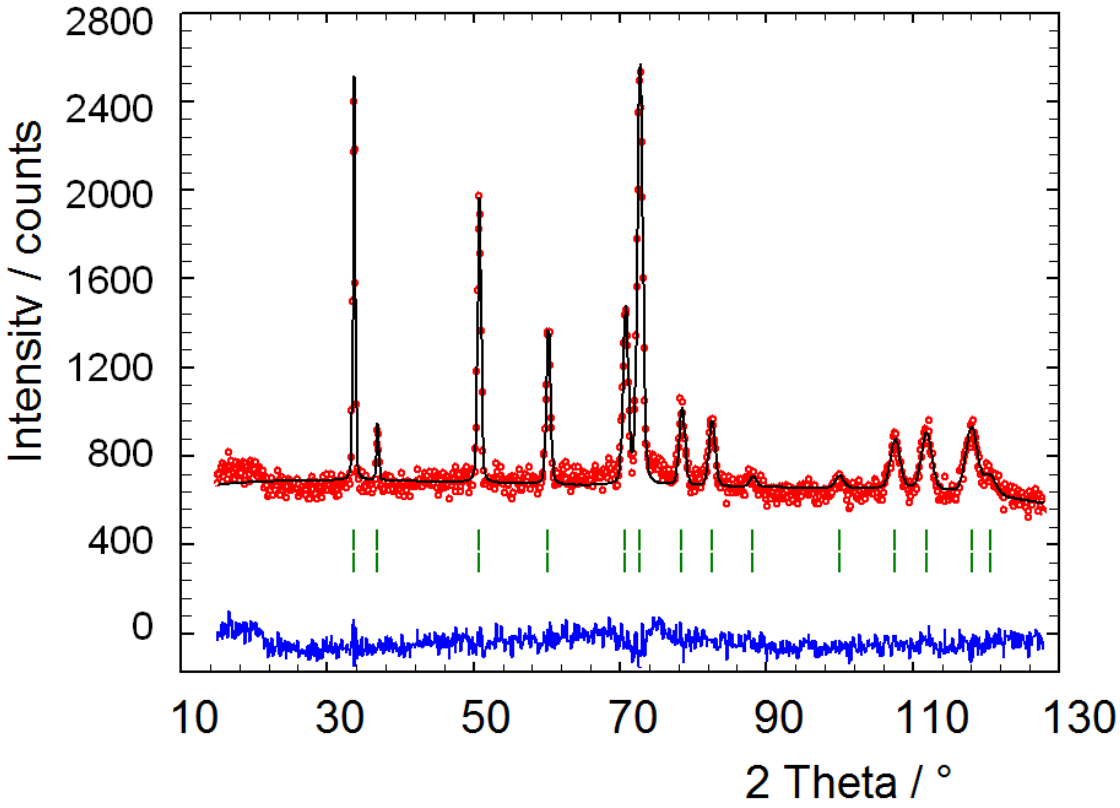

Figure S3: Rietveld refinement of the nuclear and magnetic structure of $^{154}SmCo_5$ based on neutron powder diffraction data (D1B, λ = 2.5218(3) Å, T = 700 K); from top to bottom: measured (black) and calculated (red) diffraction pattern, Bragg markers of structural and magnetic phase, difference diffraction pattern (blue).

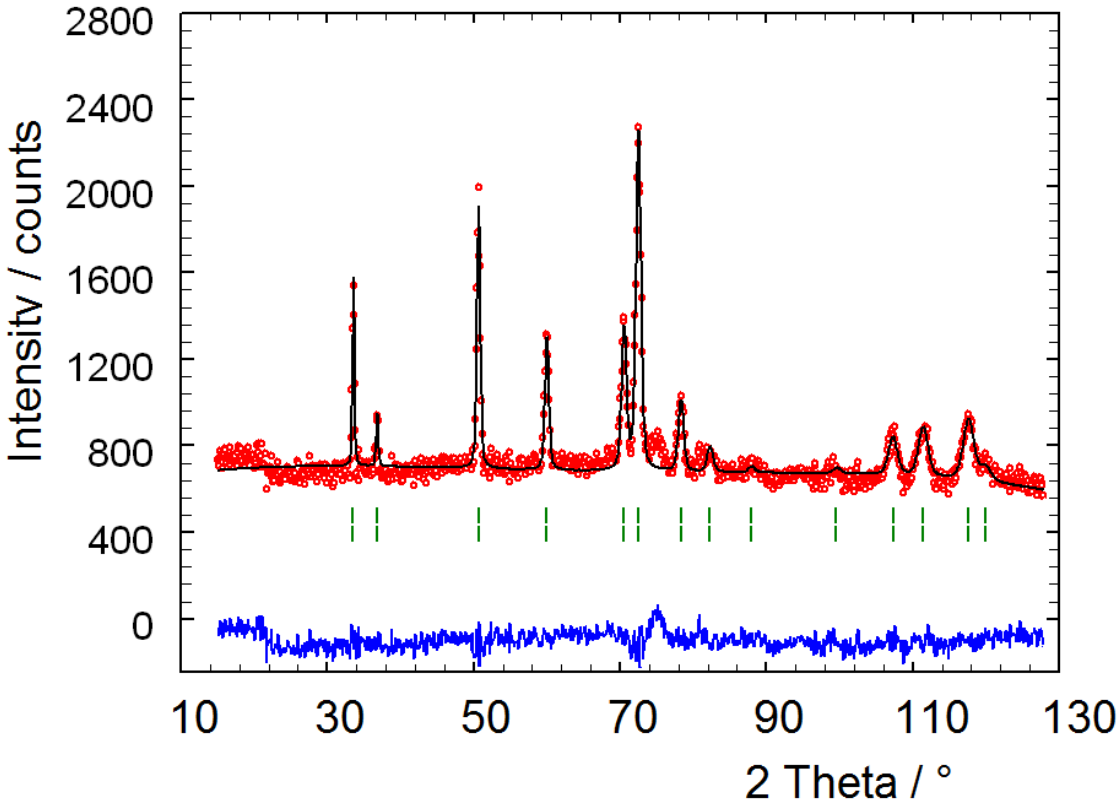

Figure S4: Rietveld refinement of the nuclear and magnetic structure of $^{154}SmCo_5$ based on neutron powder diffraction data (D1B, λ = 2.5218(3) Å, T = 907 K); from top to bottom: measured (black) and calculated (red) diffraction pattern, Bragg markers of structural and magnetic phase, difference diffraction pattern (blue).

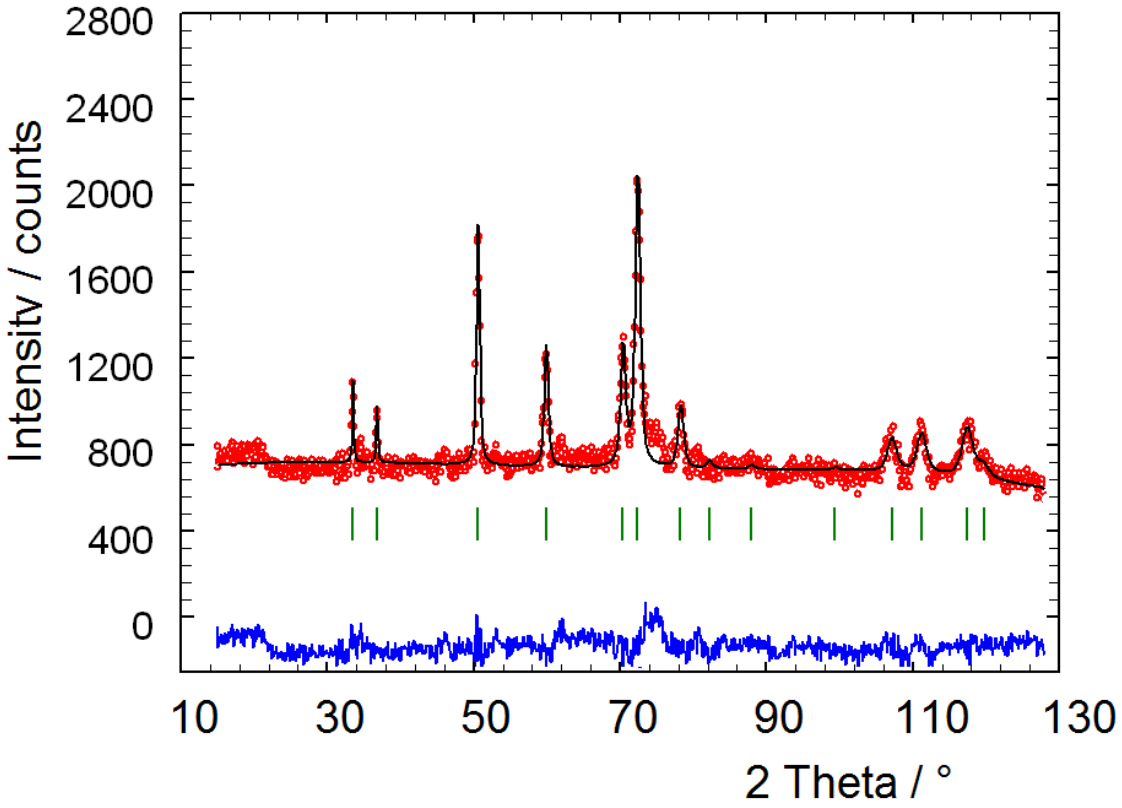

Figure S5: Rietveld refinement of the nuclear and magnetic structure of $^{154}SmCo_5$ based on neutron powder diffraction data (D1B, λ = 2.5218(3) Å, T = 1029 K); from top to bottom: measured (black) and calculated (red) diffraction pattern, Bragg markers of structural and magnetic phase, difference diffraction pattern (blue).

Table S1: Magnetic moment μ in Bohr magnetons μ_B along crystallographic [001] of Sm, Co1, Co2 in $^{154}SmCo_5$ for 5.4 K ≤ T ≤ 318.8 K (cryostate) as determined by sequential refinement on neutron powder diffraction data and their estimated standard uncertainties σ.

T / K	μ(Sm)/μ_B	$\sigma(\mu$(Sm))/μ_B	μ(Co1)/μ_B	$\sigma(\mu$(Co1))/μ_B	μ(Co2)/μ_B	$\sigma(\mu$(Co2))/μ_B
5.4	0.99	0.08	2.22	0.07	2.24	0.07
6.6	0.90	0.08	2.14	0.07	2.17	0.06
5.0	0.94	0.08	2.23	0.07	2.18	0.07
6.2	0.83	0.08	2.11	0.07	2.15	0.07
7.4	0.92	0.08	2.30	0.07	2.15	0.07
8.7	1.03	0.08	2.21	0.07	2.27	0.07
9.9	0.93	0.08	2.18	0.07	2.20	0.06
11.1	0.88	0.08	2.20	0.07	2.12	0.07
12.4	0.94	0.08	2.19	0.07	2.21	0.07
13.6	0.98	0.08	2.18	0.07	2.26	0.07
14.9	0.92	0.08	2.19	0.07	2.22	0.07
16.1	0.84	0.08	2.12	0.07	2.19	0.07
17.3	1.02	0.08	2.26	0.07	2.22	0.07
18.6	0.94	0.08	2.20	0.07	2.20	0.06
19.8	0.90	0.08	2.14	0.07	2.18	0.07
21.0	0.82	0.08	2.13	0.07	2.11	0.07
22.3	0.85	0.08	2.14	0.08	2.14	0.07
23.5	0.86	0.08	2.15	0.07	2.17	0.07
24.7	0.98	0.08	2.22	0.07	2.25	0.07
26.0	0.93	0.08	2.20	0.07	2.16	0.07
27.2	0.98	0.08	2.23	0.07	2.24	0.07
28.4	0.93	0.08	2.28	0.07	2.16	0.07
29.7	0.81	0.08	2.09	0.07	2.16	0.07
30.9	0.95	0.08	2.28	0.07	2.15	0.06
32.1	0.95	0.08	2.22	0.07	2.18	0.07
33.3	0.91	0.08	2.18	0.07	2.12	0.07
34.6	0.98	0.08	2.24	0.07	2.18	0.07
35.8	0.88	0.08	2.14	0.07	2.22	0.07
37.0	0.98	0.08	2.23	0.07	2.25	0.07

T / K	μ(Sm)/μ_B	$\sigma(\mu$(Sm))/μ_B	μ(Co1)/μ_B	$\sigma(\mu$(Co1))/μ_B	μ(Co2)/μ_B	$\sigma(\mu$(Co2))/μ_B
38.2	0.96	0.08	2.30	0.07	2.21	0.07
39.5	0.90	0.08	2.17	0.08	2.16	0.07
40.7	0.88	0.08	2.17	0.07	2.16	0.07
41.9	0.90	0.08	2.21	0.07	2.13	0.06
43.1	0.86	0.08	2.10	0.07	2.20	0.07
44.4	0.90	0.08	2.19	0.08	2.16	0.07
45.6	0.88	0.08	2.14	0.07	2.19	0.07
46.8	0.93	0.08	2.17	0.07	2.25	0.06
48.1	0.96	0.08	2.19	0.07	2.23	0.06
49.3	0.96	0.08	2.24	0.07	2.20	0.07
50.5	0.91	0.08	2.15	0.07	2.17	0.07
51.8	0.98	0.08	2.24	0.07	2.23	0.07
53.0	0.87	0.08	2.04	0.08	2.22	0.07
54.2	0.96	0.08	2.19	0.08	2.24	0.07
55.4	0.91	0.08	2.13	0.07	2.23	0.07
56.7	0.92	0.08	2.19	0.07	2.19	0.07
57.9	0.98	0.08	2.21	0.07	2.27	0.07
59.1	0.98	0.08	2.26	0.07	2.22	0.06
60.4	0.97	0.08	2.20	0.07	2.22	0.07
61.6	0.92	0.08	2.20	0.07	2.17	0.07
62.8	0.93	0.08	2.23	0.08	2.19	0.07
64.1	0.85	0.08	2.14	0.08	2.17	0.07
65.3	0.94	0.08	2.26	0.08	2.18	0.07
66.5	0.94	0.08	2.23	0.07	2.17	0.07
67.8	0.92	0.08	2.19	0.07	2.20	0.07
69.0	0.96	0.08	2.21	0.07	2.20	0.06
70.2	0.85	0.08	2.17	0.07	2.13	0.07
71.5	0.95	0.08	2.25	0.07	2.18	0.07
72.7	0.97	0.08	2.25	0.08	2.26	0.07
73.9	0.98	0.08	2.26	0.08	2.25	0.07
75.2	1.03	0.08	2.21	0.07	2.31	0.07
76.4	1.01	0.08	2.31	0.07	2.21	0.07

T / K	μ(Sm)/μ_B	$\sigma(\mu$(Sm))/μ_B	μ(Co1)/μ_B	$\sigma(\mu$(Co1))/μ_B	μ(Co2)/μ_B	$\sigma(\mu$(Co2))/μ_B
77.7	1.08	0.08	2.30	0.08	2.35	0.07
78.9	0.92	0.08	2.24	0.07	2.16	0.07
80.1	0.97	0.08	2.19	0.07	2.26	0.07
81.4	0.92	0.08	2.21	0.08	2.18	0.07
82.6	0.89	0.08	2.20	0.07	2.18	0.07
83.8	0.93	0.08	2.24	0.07	2.17	0.07
85.1	1.04	0.08	2.35	0.07	2.25	0.07
86.3	0.87	0.08	2.17	0.08	2.18	0.07
87.6	0.89	0.08	2.23	0.07	2.16	0.07
88.8	0.90	0.08	2.19	0.08	2.18	0.07
90.0	0.94	0.08	2.20	0.07	2.20	0.07
91.3	0.93	0.08	2.23	0.07	2.17	0.07
92.5	0.97	0.08	2.21	0.08	2.28	0.07
93.8	0.91	0.08	2.24	0.07	2.17	0.07
95.0	0.85	0.08	2.22	0.07	2.10	0.07
96.2	0.94	0.08	2.21	0.08	2.22	0.07
97.5	0.87	0.08	2.18	0.07	2.12	0.07
98.7	0.99	0.08	2.27	0.08	2.25	0.07
99.9	0.94	0.08	2.18	0.07	2.23	0.07
101.2	0.89	0.08	2.17	0.07	2.19	0.07
102.3	0.86	0.08	2.22	0.08	2.18	0.07
103.5	0.86	0.08	2.16	0.07	2.14	0.07
104.8	0.97	0.08	2.23	0.07	2.26	0.07
106.0	0.87	0.08	2.17	0.08	2.21	0.07
107.2	0.98	0.08	2.32	0.07	2.14	0.07
108.5	0.96	0.08	2.19	0.08	2.28	0.07
109.7	0.92	0.08	2.25	0.08	2.17	0.07
111.0	0.84	0.08	2.17	0.07	2.15	0.06
112.2	0.93	0.08	2.21	0.07	2.22	0.07
113.4	0.91	0.08	2.28	0.07	2.13	0.07
114.7	0.89	0.08	2.21	0.08	2.16	0.07
115.9	0.82	0.08	2.09	0.07	2.11	0.07

T / K	μ(Sm)/μ_B	$\sigma(\mu$(Sm))/μ_B	μ(Co1)/μ_B	$\sigma(\mu$(Co1))/μ_B	μ(Co2)/μ_B	$\sigma(\mu$(Co2))/μ_B
117.2	0.84	0.08	2.13	0.08	2.15	0.07
118.4	0.87	0.08	2.23	0.08	2.14	0.07
119.7	0.86	0.08	2.13	0.08	2.20	0.07
120.9	0.84	0.08	2.15	0.08	2.08	0.07
122.1	0.89	0.08	2.21	0.08	2.18	0.07
123.4	0.92	0.08	2.22	0.07	2.20	0.07
124.6	0.90	0.08	2.13	0.08	2.22	0.07
125.9	0.93	0.08	2.22	0.08	2.21	0.07
127.1	0.88	0.08	2.19	0.07	2.14	0.07
128.3	0.92	0.08	2.13	0.07	2.22	0.07
129.6	0.99	0.09	2.21	0.08	2.29	0.07
130.8	0.88	0.08	2.18	0.08	2.13	0.07
132.0	0.88	0.08	2.24	0.08	2.11	0.07
133.3	0.80	0.08	2.08	0.08	2.15	0.07
134.5	0.89	0.08	2.16	0.08	2.26	0.07
135.8	0.91	0.08	2.17	0.07	2.20	0.07
137.0	0.88	0.08	2.24	0.07	2.18	0.07
138.2	0.75	0.08	2.12	0.07	2.08	0.06
139.5	0.92	0.08	2.20	0.07	2.23	0.07
140.7	0.90	0.08	2.14	0.08	2.25	0.07
142.0	0.86	0.08	2.17	0.07	2.14	0.07
143.2	0.97	0.08	2.27	0.08	2.29	0.07
144.4	0.94	0.08	2.21	0.08	2.23	0.07
145.7	0.91	0.08	2.19	0.07	2.22	0.07
146.9	0.88	0.08	2.27	0.08	2.16	0.07
148.2	0.97	0.08	2.28	0.07	2.21	0.07
149.4	0.85	0.08	2.18	0.08	2.18	0.07
150.6	0.81	0.08	2.18	0.07	2.17	0.07
151.9	0.92	0.08	2.24	0.08	2.23	0.07
153.1	0.87	0.08	2.24	0.08	2.18	0.07
154.4	0.87	0.09	2.20	0.08	2.16	0.07
155.6	0.89	0.08	2.18	0.07	2.20	0.07

T / K	μ(Sm)/μ_B	$\sigma(\mu$(Sm))/μ_B	μ(Co1)/μ_B	$\sigma(\mu$(Co1))/μ_B	μ(Co2)/μ_B	$\sigma(\mu$(Co2))/μ_B
156.8	0.87	0.08	2.22	0.08	2.12	0.07
158.1	0.86	0.08	2.21	0.08	2.18	0.07
159.3	0.80	0.08	2.14	0.08	2.15	0.07
160.5	0.87	0.08	2.19	0.07	2.18	0.07
161.8	0.86	0.08	2.18	0.08	2.19	0.07
163.0	0.80	0.09	2.13	0.08	2.16	0.07
164.3	0.80	0.09	2.08	0.08	2.18	0.07
165.5	0.81	0.08	2.10	0.08	2.23	0.07
166.7	0.91	0.08	2.20	0.08	2.17	0.07
168.0	0.85	0.09	2.20	0.08	2.20	0.07
169.2	0.80	0.08	2.15	0.07	2.11	0.07
170.5	0.84	0.08	2.18	0.07	2.14	0.07
171.7	0.79	0.08	2.12	0.07	2.12	0.07
172.9	0.78	0.08	2.12	0.07	2.13	0.07
174.2	0.75	0.08	2.09	0.08	2.10	0.07
175.4	0.77	0.08	2.13	0.08	2.14	0.07
176.7	0.80	0.08	2.17	0.08	2.15	0.07
177.9	0.74	0.08	2.11	0.08	2.09	0.07
179.2	0.85	0.08	2.15	0.08	2.21	0.07
180.4	0.83	0.09	2.13	0.08	2.18	0.07
181.7	0.84	0.08	2.20	0.08	2.12	0.07
182.9	0.72	0.08	2.11	0.08	2.12	0.07
184.1	0.80	0.08	2.11	0.08	2.15	0.07
185.4	0.81	0.09	2.09	0.08	2.18	0.07
186.6	0.82	0.08	2.14	0.08	2.15	0.07
187.9	0.90	0.08	2.25	0.08	2.14	0.07
189.1	0.80	0.09	2.15	0.08	2.07	0.07
190.4	0.83	0.08	2.21	0.08	2.17	0.07
191.6	0.85	0.08	2.21	0.08	2.12	0.07
192.8	0.90	0.08	2.26	0.08	2.22	0.07
194.1	0.83	0.09	2.14	0.08	2.18	0.07
195.3	0.73	0.09	2.12	0.08	2.11	0.07

T / K	μ(Sm)/μ_B	$\sigma(\mu$(Sm))/μ_B	μ(Co1)/μ_B	$\sigma(\mu$(Co1))/μ_B	μ(Co2)/μ_B	$\sigma(\mu$(Co2))/μ_B
196.6	0.89	0.09	2.24	0.08	2.21	0.08
197.8	0.85	0.09	2.24	0.08	2.21	0.07
199.0	0.87	0.09	2.23	0.08	2.23	0.07
200.3	0.96	0.08	2.28	0.07	2.21	0.07
201.5	0.84	0.08	2.17	0.08	2.22	0.07
202.8	0.86	0.08	2.14	0.07	2.23	0.07
204.0	0.88	0.09	2.25	0.08	2.16	0.07
205.2	0.78	0.08	2.11	0.08	2.18	0.07
206.5	0.78	0.09	2.13	0.08	2.13	0.07
207.7	0.74	0.08	2.13	0.08	2.08	0.07
209.0	0.93	0.08	2.22	0.08	2.24	0.07
210.2	0.78	0.08	2.13	0.08	2.14	0.07
211.5	0.79	0.09	2.14	0.08	2.13	0.07
212.7	0.82	0.08	2.22	0.08	2.15	0.07
214.0	0.76	0.08	2.21	0.08	2.12	0.07
215.2	0.76	0.09	2.19	0.08	2.10	0.07
216.4	0.73	0.08	2.06	0.08	2.18	0.07
217.7	0.78	0.09	2.16	0.08	2.18	0.07
218.9	0.68	0.08	2.11	0.08	2.09	0.07
220.1	0.77	0.09	2.18	0.08	2.11	0.07
221.4	0.65	0.09	2.06	0.08	2.07	0.07
222.6	0.75	0.08	2.12	0.08	2.15	0.07
223.9	0.81	0.08	2.24	0.08	2.15	0.07
225.1	0.69	0.09	2.09	0.08	2.06	0.07
226.3	0.73	0.09	2.12	0.08	2.16	0.07
227.6	0.77	0.09	2.17	0.08	2.18	0.08
228.8	0.77	0.08	2.18	0.08	2.19	0.07
230.0	0.77	0.09	2.12	0.08	2.23	0.07
231.3	0.71	0.08	2.13	0.08	2.10	0.07
232.5	0.72	0.09	2.18	0.08	2.05	0.07
233.8	0.79	0.09	2.13	0.08	2.21	0.08
235.0	0.82	0.08	2.21	0.08	2.22	0.07

T / K	μ(Sm)/μ_B	$\sigma(\mu$(Sm))/μ_B	μ(Co1)/μ_B	$\sigma(\mu$(Co1))/μ_B	μ(Co2)/μ_B	$\sigma(\mu$(Co2))/μ_B
236.2	0.69	0.08	2.09	0.08	2.13	0.07
237.5	0.77	0.09	2.21	0.08	2.19	0.07
238.7	0.74	0.09	2.18	0.08	2.12	0.07
239.9	0.68	0.09	2.11	0.08	2.09	0.07
241.2	0.84	0.09	2.18	0.08	2.23	0.07
242.4	0.64	0.09	2.06	0.08	2.06	0.07
243.7	0.62	0.09	2.09	0.08	2.07	0.07
244.9	0.65	0.09	2.05	0.08	2.13	0.07
246.1	0.71	0.09	2.09	0.08	2.12	0.07
247.4	0.78	0.08	2.18	0.08	2.22	0.07
248.6	0.71	0.09	2.22	0.08	2.07	0.08
249.8	0.59	0.09	2.00	0.08	2.07	0.07
251.1	0.81	0.08	2.23	0.08	2.18	0.07
252.3	0.81	0.09	2.17	0.08	2.26	0.07
253.6	0.62	0.09	2.01	0.08	2.11	0.07
254.8	0.69	0.09	2.17	0.08	2.08	0.07
256.0	0.63	0.08	2.12	0.08	2.04	0.07
257.3	0.68	0.09	2.14	0.08	2.07	0.07
258.5	0.67	0.08	2.07	0.08	2.12	0.07
259.8	0.61	0.09	2.08	0.08	2.08	0.07
261.0	0.64	0.09	2.12	0.08	2.07	0.07
262.2	0.78	0.09	2.24	0.08	2.15	0.07
263.5	0.68	0.08	2.17	0.08	2.07	0.07
264.7	0.66	0.09	2.09	0.08	2.10	0.07
266.0	0.68	0.08	2.08	0.08	2.12	0.07
267.2	0.79	0.08	2.26	0.08	2.15	0.07
268.4	0.62	0.09	2.11	0.08	2.11	0.07
269.7	0.69	0.09	2.11	0.08	2.12	0.07
270.9	0.69	0.08	2.20	0.08	2.10	0.07
272.2	0.70	0.08	2.18	0.08	2.07	0.07
273.4	0.55	0.09	2.01	0.08	2.06	0.07
274.7	0.66	0.08	2.11	0.08	2.13	0.07

T / K	μ(Sm)/μ_B	$\sigma(\mu$(Sm))/μ_B	μ(Co1)/μ_B	$\sigma(\mu$(Co1))/μ_B	μ(Co2)/μ_B	$\sigma(\mu$(Co2))/μ_B
275.9	0.54	0.09	2.08	0.08	1.98	0.07
277.1	0.69	0.09	2.11	0.08	2.14	0.07
278.4	0.62	0.09	2.06	0.08	2.06	0.07
279.6	0.66	0.08	2.17	0.08	2.13	0.07
280.8	0.65	0.09	2.15	0.08	2.09	0.07
282.1	0.78	0.09	2.26	0.08	2.19	0.08
283.3	0.66	0.09	2.14	0.08	2.05	0.07
284.5	0.59	0.09	2.19	0.08	2.00	0.07
285.8	0.65	0.09	2.16	0.08	2.06	0.07
287.0	0.69	0.09	2.18	0.08	2.12	0.07
288.2	0.57	0.09	2.06	0.08	2.04	0.07
289.4	0.56	0.09	2.00	0.08	2.07	0.07
290.7	0.67	0.09	2.15	0.08	2.11	0.07
291.9	0.65	0.09	2.09	0.08	2.09	0.07
293.2	0.64	0.09	2.12	0.08	2.06	0.07
294.4	0.62	0.09	2.03	0.08	2.18	0.07
295.6	0.73	0.09	2.13	0.08	2.18	0.08
296.8	0.62	0.10	2.03	0.09	2.14	0.08
298.1	0.65	0.09	2.04	0.08	2.18	0.07
299.3	0.65	0.09	2.13	0.08	2.14	0.07
300.5	0.62	0.09	2.12	0.08	2.08	0.07
301.8	0.65	0.09	2.10	0.08	2.06	0.07
303.0	0.55	0.09	2.08	0.08	2.01	0.07
304.2	0.58	0.09	2.09	0.09	2.03	0.08
305.5	0.66	0.09	2.12	0.08	2.13	0.07
306.7	0.63	0.09	2.10	0.08	2.10	0.07
307.9	0.72	0.09	2.17	0.08	2.09	0.07
309.2	0.53	0.09	2.07	0.08	1.99	0.07
310.4	0.67	0.09	2.16	0.08	2.06	0.07
311.6	0.61	0.09	2.11	0.08	2.05	0.07
312.9	0.57	0.09	2.08	0.08	2.01	0.07
314.1	0.56	0.09	2.06	0.08	2.07	0.07

T / K	μ(Sm)/μ_B	$\sigma(\mu$(Sm))/μ_B	μ(Co1)/μ_B	$\sigma(\mu$(Co1))/μ_B	μ(Co2)/μ_B	$\sigma(\mu$(Co2))/μ_B
315.3	0.71	0.09	2.22	0.08	2.11	0.07
316.6	0.52	0.09	1.97	0.09	2.01	0.07
317.8	0.64	0.09	2.10	0.09	2.12	0.07
318.8	0.48	0.09	2.03	0.09	1.99	0.07

Table S2: Magnetic moment μ in Bohr magnetons μ_B along crystallographic [001] of Sm, Co1, Co2 in $^{154}SmCo_5$ for 294.5 K ≤ T ≤ 1037 K (furnace) as determined by sequential refinement on neutron powder diffraction data and their estimated standard uncertainties σ.

T / K	μ(Sm)/μ_B	$\sigma(\mu$(Sm))/μ_B	μ(Co1)/μ_B	$\sigma(\mu$(Co1))/μ_B	μ(Co2)/μ_B	$\sigma(\mu$(Co2))/μ_B
294.5	0.60	0.12	2.01	0.11	1.86	0.09
301.6	0.67	0.11	2.08	0.10	1.88	0.09
307.5	0.67	0.12	2.06	0.11	1.96	0.09
312.6	0.59	0.12	1.97	0.11	1.96	0.09
317.5	0.65	0.12	2.04	0.11	1.95	0.10
322.1	0.69	0.12	2.05	0.10	1.94	0.09
326.6	0.67	0.11	2.02	0.10	1.94	0.09
331.0	0.66	0.12	2.02	0.10	1.95	0.09
335.3	0.66	0.12	2.07	0.11	1.87	0.09
339.5	0.63	0.13	1.95	0.12	2.03	0.10
343.6	0.58	0.13	1.96	0.11	1.90	0.10
348.0	0.74	0.12	2.14	0.11	2.01	0.09
352.1	0.48	0.12	1.90	0.11	1.86	0.09
356.3	0.59	0.12	2.00	0.11	1.93	0.09
360.4	0.57	0.12	2.01	0.11	1.91	0.09
364.5	0.54	0.12	1.96	0.11	1.88	0.09
368.5	0.63	0.12	2.02	0.11	1.97	0.09
372.5	0.53	0.12	1.99	0.11	1.93	0.09
376.5	0.31	0.13	1.82	0.12	1.81	0.09
380.4	0.67	0.12	2.11	0.11	1.94	0.09
384.5	0.62	0.12	2.01	0.11	1.95	0.10
388.5	0.54	0.12	1.96	0.11	1.85	0.10
392.5	0.40	0.12	1.83	0.11	1.83	0.09
396.6	0.55	0.12	2.02	0.11	1.92	0.10
400.8	0.48	0.13	1.99	0.11	1.82	0.10
404.8	0.49	0.12	1.99	0.11	1.84	0.10
408.8	0.41	0.12	1.88	0.11	1.81	0.09
412.9	0.41	0.13	1.85	0.11	1.81	0.09
416.9	0.53	0.12	1.94	0.11	1.89	0.09

T / K	μ(Sm)/μ_B	$\sigma(\mu$(Sm))/μ_B	μ(Co1)/μ_B	$\sigma(\mu$(Co1))/μ_B	μ(Co2)/μ_B	$\sigma(\mu$(Co2))/μ_B
420.9	0.40	0.12	1.93	0.11	1.76	0.09
424.9	0.64	0.12	2.03	0.11	1.97	0.10
428.8	0.44	0.13	1.94	0.12	1.81	0.10
432.8	0.52	0.12	2.02	0.11	1.82	0.10
436.8	0.59	0.12	2.02	0.11	1.90	0.10
440.8	0.39	0.13	1.84	0.12	1.85	0.10
444.9	0.48	0.14	1.91	0.13	1.91	0.10
448.9	0.48	0.13	1.85	0.12	1.86	0.10
452.9	0.41	0.13	1.87	0.12	1.82	0.10
456.8	0.61	0.12	2.01	0.11	1.89	0.09
460.8	0.49	0.13	1.89	0.12	1.87	0.10
464.8	0.53	0.12	2.02	0.11	1.80	0.09
468.5	0.48	0.13	1.89	0.11	1.86	0.09
472.5	0.55	0.13	2.02	0.12	1.83	0.10
476.5	0.50	0.12	1.99	0.11	1.78	0.09
480.5	0.44	0.13	1.83	0.12	1.83	0.10
484.5	0.48	0.13	1.82	0.12	1.88	0.10
488.5	0.38	0.13	1.85	0.12	1.86	0.10
492.6	0.56	0.13	1.95	0.12	1.90	0.10
496.6	0.55	0.12	2.02	0.11	1.79	0.09
500.6	0.47	0.13	1.89	0.12	1.79	0.10
504.5	0.50	0.13	1.94	0.12	1.82	0.10
508.5	0.32	0.14	1.85	0.12	1.69	0.10
512.5	0.47	0.14	1.80	0.12	1.85	0.10
516.7	0.48	0.13	1.92	0.12	1.79	0.10
520.7	0.48	0.13	1.89	0.12	1.78	0.10
524.5	0.41	0.13	1.90	0.12	1.77	0.10
528.5	0.36	0.14	1.75	0.13	1.78	0.10
532.7	0.34	0.14	1.70	0.12	1.74	0.10
536.7	0.47	0.13	1.85	0.12	1.78	0.10
540.8	0.43	0.14	1.95	0.12	1.68	0.10
544.8	0.36	0.13	1.87	0.12	1.70	0.10

T / K	μ(Sm)/μ_B	$\sigma(\mu$(Sm))/μ_B	μ(Co1)/μ_B	$\sigma(\mu$(Co1))/μ_B	μ(Co2)/μ_B	$\sigma(\mu$(Co2))/μ_B
549.0	0.37	0.14	1.78	0.13	1.75	0.10
553.0	0.49	0.14	1.71	0.13	1.79	0.10
557.0	0.33	0.14	1.72	0.13	1.72	0.10
561.0	0.40	0.14	1.84	0.12	1.69	0.10
565.0	0.51	0.14	1.83	0.13	1.82	0.10
569.2	0.40	0.14	1.84	0.13	1.67	0.10
573.3	0.45	0.13	1.84	0.12	1.68	0.10
577.3	0.37	0.14	1.82	0.13	1.63	0.10
581.5	0.42	0.14	1.86	0.13	1.64	0.10
585.7	0.33	0.14	1.77	0.13	1.69	0.10
589.8	0.44	0.14	1.77	0.13	1.77	0.10
594.0	0.30	0.15	1.74	0.13	1.62	0.10
598.2	0.16	0.16	1.55	0.14	1.64	0.10
599.3	0.30	0.15	1.75	0.13	1.64	0.10
598.8	0.42	0.15	1.69	0.13	1.70	0.10
607.8	0.33	0.14	1.73	0.13	1.62	0.10
616.8	0.43	0.15	1.71	0.14	1.74	0.11
624.7	0.40	0.14	1.82	0.13	1.61	0.10
632.5	0.23	0.15	1.62	0.14	1.56	0.10
641.3	0.43	0.15	1.80	0.14	1.63	0.11
649.3	0.18	0.18	1.41	0.16	1.66	0.11
657.3	0.18	0.16	1.53	0.15	1.53	0.11
665.5	0.43	0.15	1.62	0.14	1.72	0.11
674.0	0.42	0.15	1.71	0.13	1.63	0.10
682.0	0.14	0.16	1.46	0.15	1.45	0.10
689.8	0.25	0.17	1.53	0.16	1.54	0.11
698.5	0.53	0.16	1.60	0.14	1.74	0.11
706.7	0.15	0.19	1.35	0.16	1.43	0.11
714.5	0.48	0.15	1.64	0.14	1.59	0.11
722.5	0.50	0.16	1.67	0.14	1.58	0.11
730.3	0.24	0.17	1.51	0.14	1.39	0.11
739.0	0.31	0.17	1.54	0.15	1.49	0.11

T / K	μ(Sm)/μ_B	$\sigma(\mu$(Sm))/μ_B	μ(Co1)/μ_B	$\sigma(\mu$(Co1))/μ_B	μ(Co2)/μ_B	$\sigma(\mu$(Co2))/μ_B
746.7	0.58	0.16	1.69	0.14	1.55	0.12
755.0	0.19	0.18	1.30	0.16	1.36	0.11
763.8	0.56	0.16	1.73	0.14	1.44	0.12
771.5	0.48	0.18	1.45	0.16	1.54	0.12
779.5	0.50	0.17	1.53	0.15	1.45	0.12
788.5	0.45	0.19	1.40	0.16	1.49	0.12
796.5	0.41	0.18	1.39	0.16	1.40	0.12
804.3	0.36	0.20	1.35	0.17	1.32	0.12
812.5	0.35	0.20	1.26	0.18	1.39	0.12
821.2	0.51	0.19	1.33	0.17	1.39	0.13
829.0	0.66	0.18	1.44	0.16	1.44	0.13
836.8	0.55	0.19	1.41	0.16	1.38	0.13
845.8	0.64	0.18	1.47	0.15	1.39	0.13
854.0	0.37	0.21	1.26	0.17	1.16	0.13
862.0	0.54	0.19	1.39	0.16	1.21	0.13
870.2	0.43	0.22	1.18	0.18	1.16	0.14
879.0	0.57	0.19	1.33	0.15	1.18	0.13
887.0	0.62	0.20	1.16	0.17	1.29	0.13
895.0	0.55	0.21	1.31	0.16	1.07	0.14
904.0	0.59	0.22	1.18	0.17	1.01	0.15
912.3	0.87	0.20	1.29	0.16	1.08	0.14
920.3	0.71	0.22	1.19	0.17	0.97	0.15
928.3	0.74	0.24	0.98	0.19	1.16	0.14
937.3	0.69	0.26	0.93	0.19	0.93	0.16
945.3	0.89	0.25	0.98	0.18	0.92	0.16
953.3	1.24	0.24	1.00	0.17	1.04	0.15
962.0	1.09	0.27	0.93	0.17	0.76	0.18
970.5	1.09	0.28	0.84	0.19	0.82	0.18
978.5	0.93	0.31	0.73	0.20	0.69	0.20
986.8	1.13	0.27	0.92	0.17	0.75	0.19
996.0	1.21	0.30	0.79	0.19	0.76	0.19
1004	0.91	0.31	0.80	0.18	0.62	0.21

T / K	μ(Sm)/μ_B	$\sigma(\mu$(Sm))/μ_B	μ(Co1)/μ_B	$\sigma(\mu$(Co1))/μ_B	μ(Co2)/μ_B	$\sigma(\mu$(Co2))/μ_B
1012	1.03	0.36	0.89	0.19	0.48	0.25
1021	1.11	0.32	0.85	0.18	0.63	0.21
1029	1.03	0.39	0.68	0.22	0.58	0.25
1037	*1.79*	*0.40*	*0.58*	*0.17*	*0.59*	*0.20*

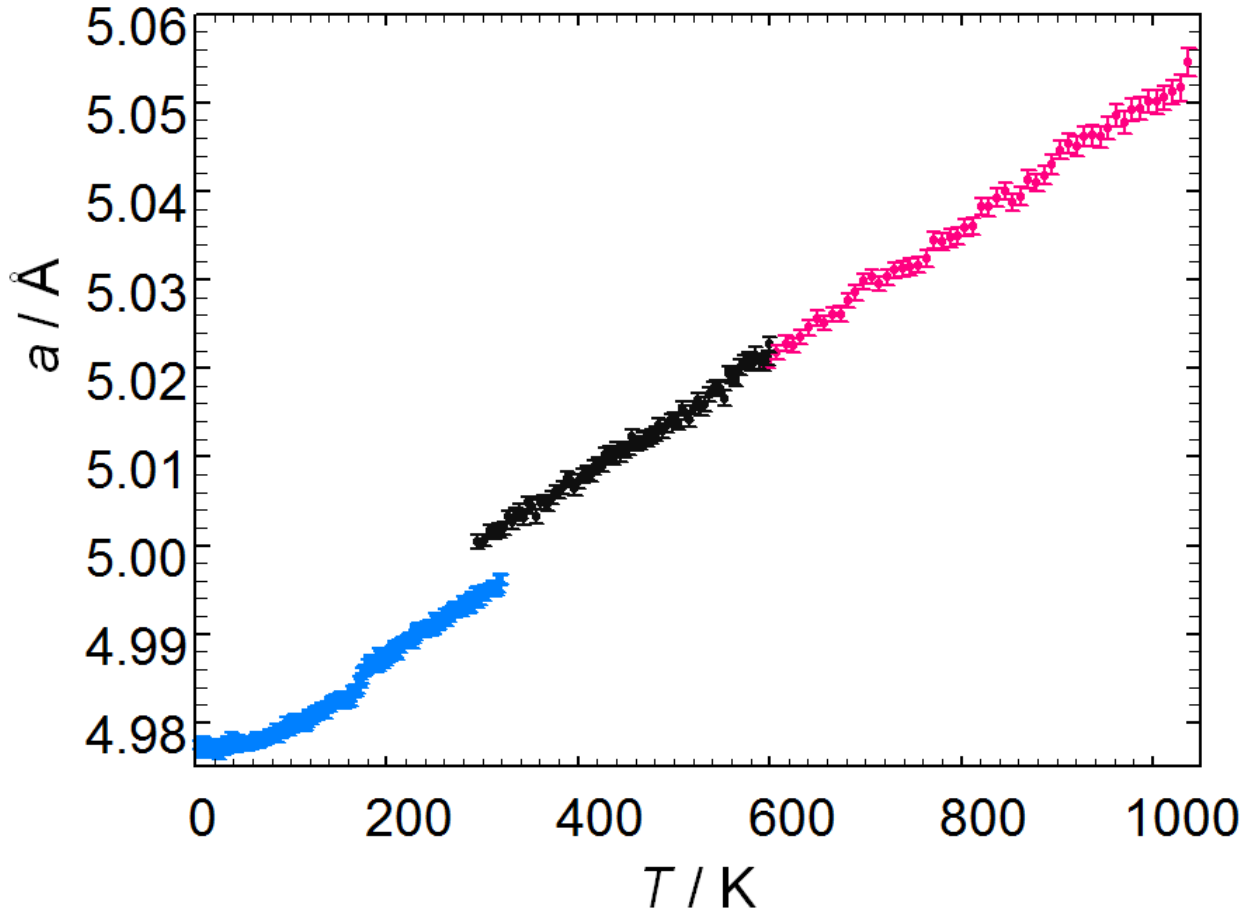

Figure S6: Lattice parameter *a* in Å of $^{154}SmCo_5$ as determined by sequential Rietveld refinement based on neutron powder diffraction data (D1B, λ = 2.5218(3) Å) in the temperature range 5.4 K ≤ *T* ≤ 318.8 K (cryostate, blue symbols), 294.5 K ≤ *T* ≤ 598.8 K (furnace, fast heating, black symbols) and 607.8 K ≤ *T* ≤ 1037 K (furnace, slow heating, red symbols). Error bars represent one estimated standard uncertainty ±σ.

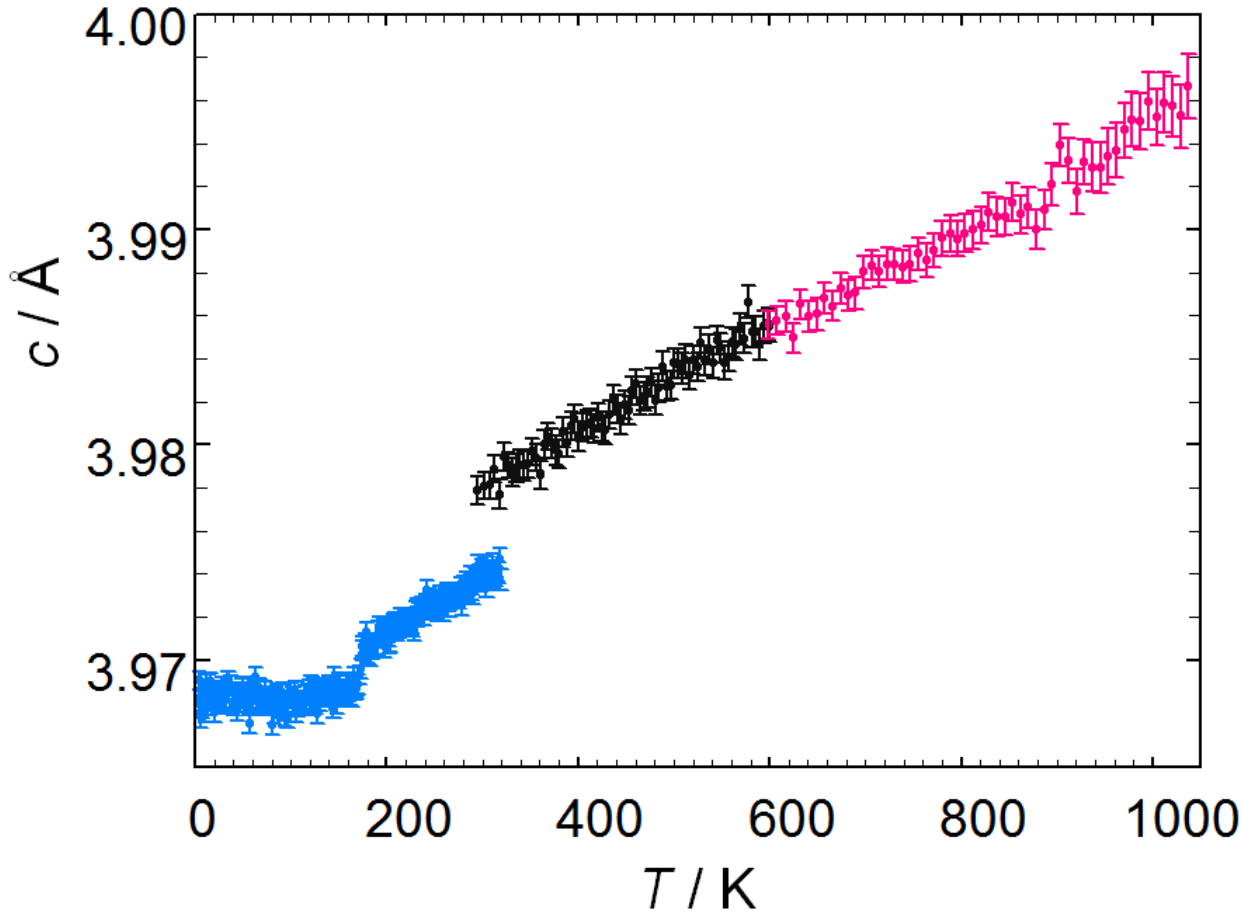

Figure S7: Lattice parameter *c* in Å of $^{154}SmCo_5$ as determined by sequential Rietveld refinement based on neutron powder diffraction data (D1B, λ = 2.5218(3) Å) in the temperature range 5.4 K ≤ *T* ≤ 318.8 K (cryostate, blue symbols), 294.5 K ≤ *T* ≤ 598.8 K (furnace, fast heating, black symbols) and 607.8 K ≤ *T* ≤ 1037 K (furnace, slow heating, red symbols). Error bars represent one estimated standard uncertainty ±σ.

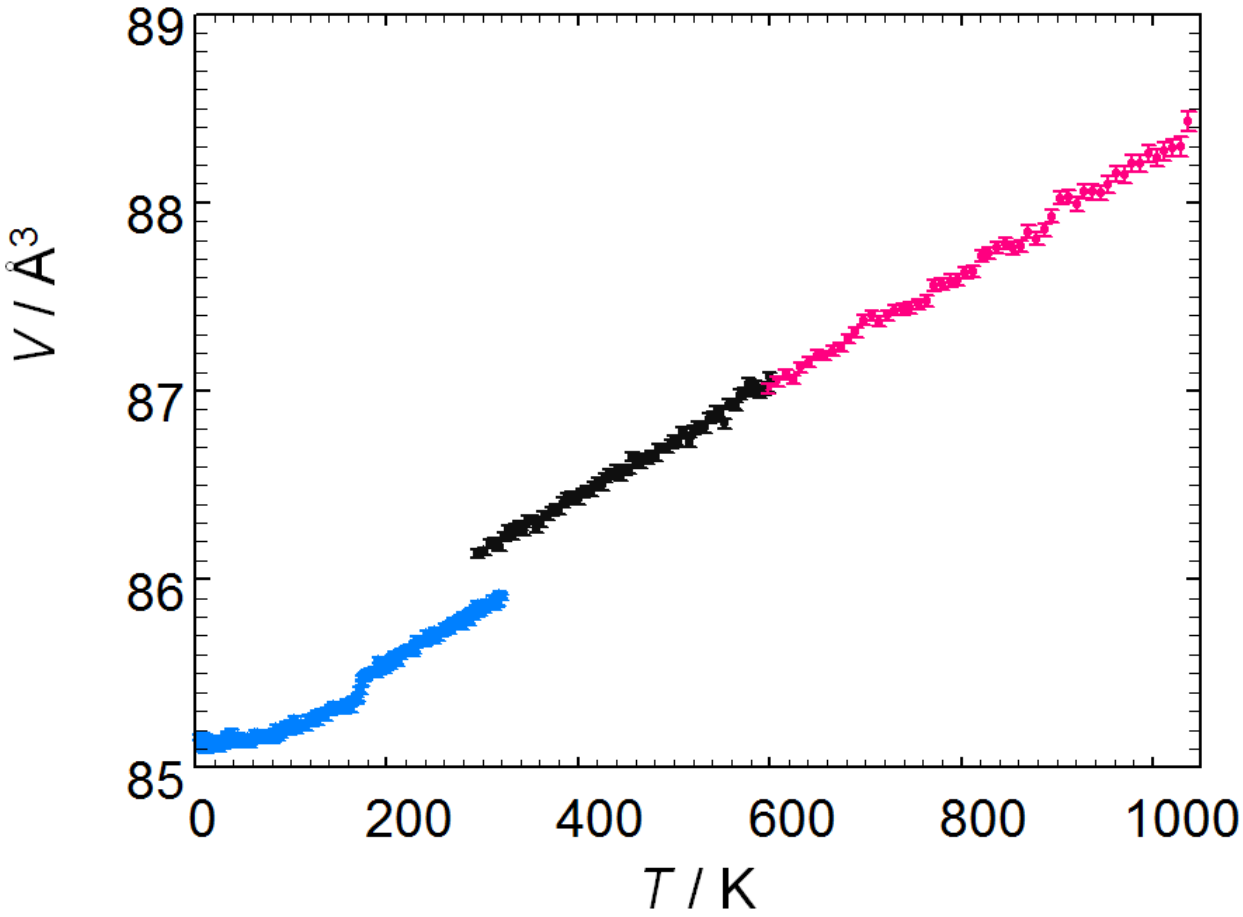

Figure S8: Unit cell volume V in Å^3 of $^{154}SmCo_5$ as determined by sequential Rietveld refinement based on neutron powder diffraction data (D1B, λ = 2.5218(3) Å) in the temperature range 5.4 K ≤ T ≤ 318.8 K (cryostate, blue symbols), 294.5 K ≤ T ≤ 598.8 K (furnace, fast heating, black symbols) and 607.8 K ≤ T ≤ 1037 K (furnace, slow heating, red symbols). Error bars represent one estimated standard uncertainty ±σ.

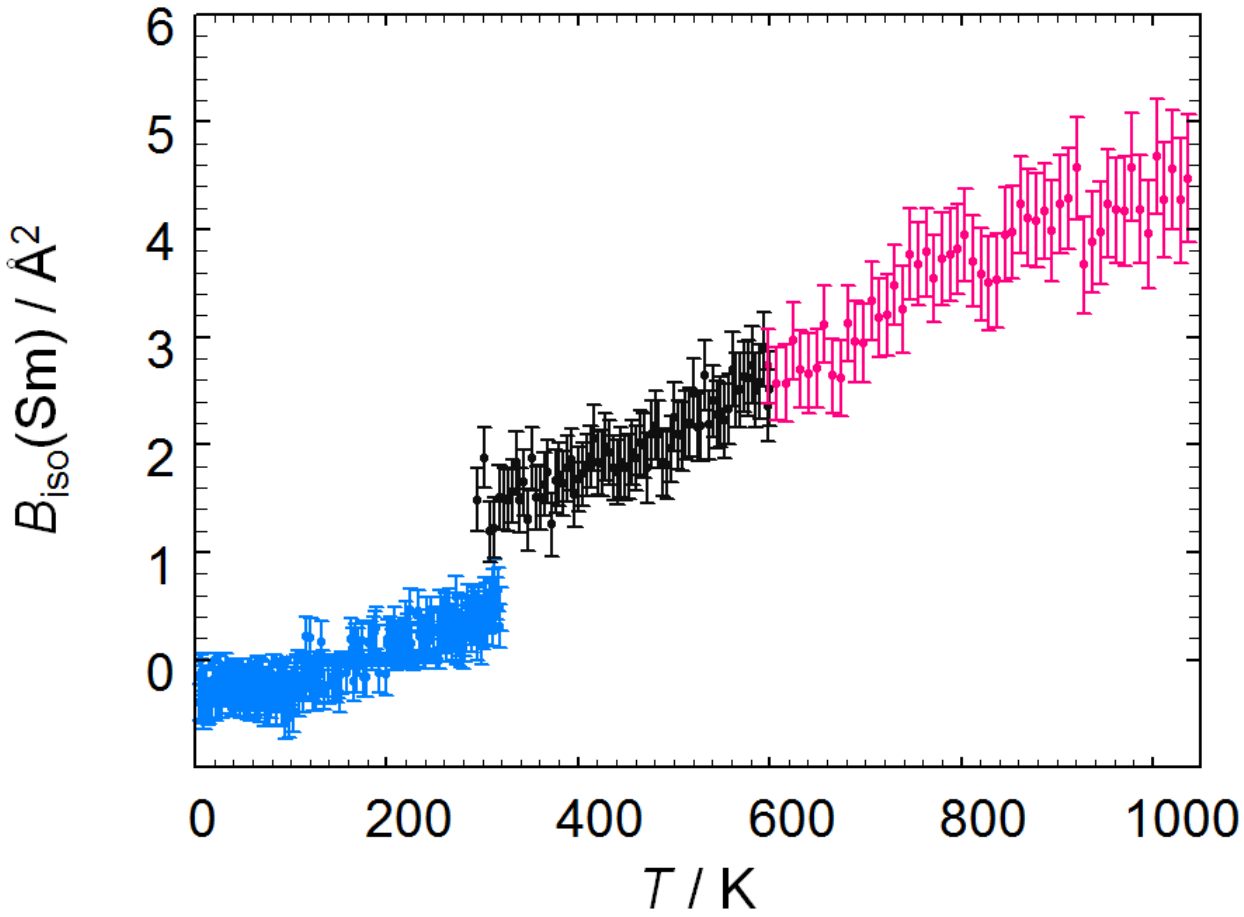

Figure S9: Thermal displacement parameter B_{iso} in Å^2 of samarium atoms in $^{154}SmCo_5$ as determined by sequential Rietveld refinement based on neutron powder diffraction data (D1B, λ = 2.5218(3) Å) in the temperature range 5.4 K ≤ T ≤ 318.8 K (cryostate, blue symbols), 294.5 K ≤ T ≤ 598.8 K (furnace, fast heating, black symbols) and 607.8 K ≤ T ≤ 1037 K (furnace, slow heating, red symbols). Error bars represent one estimated standard uncertainty ±σ.

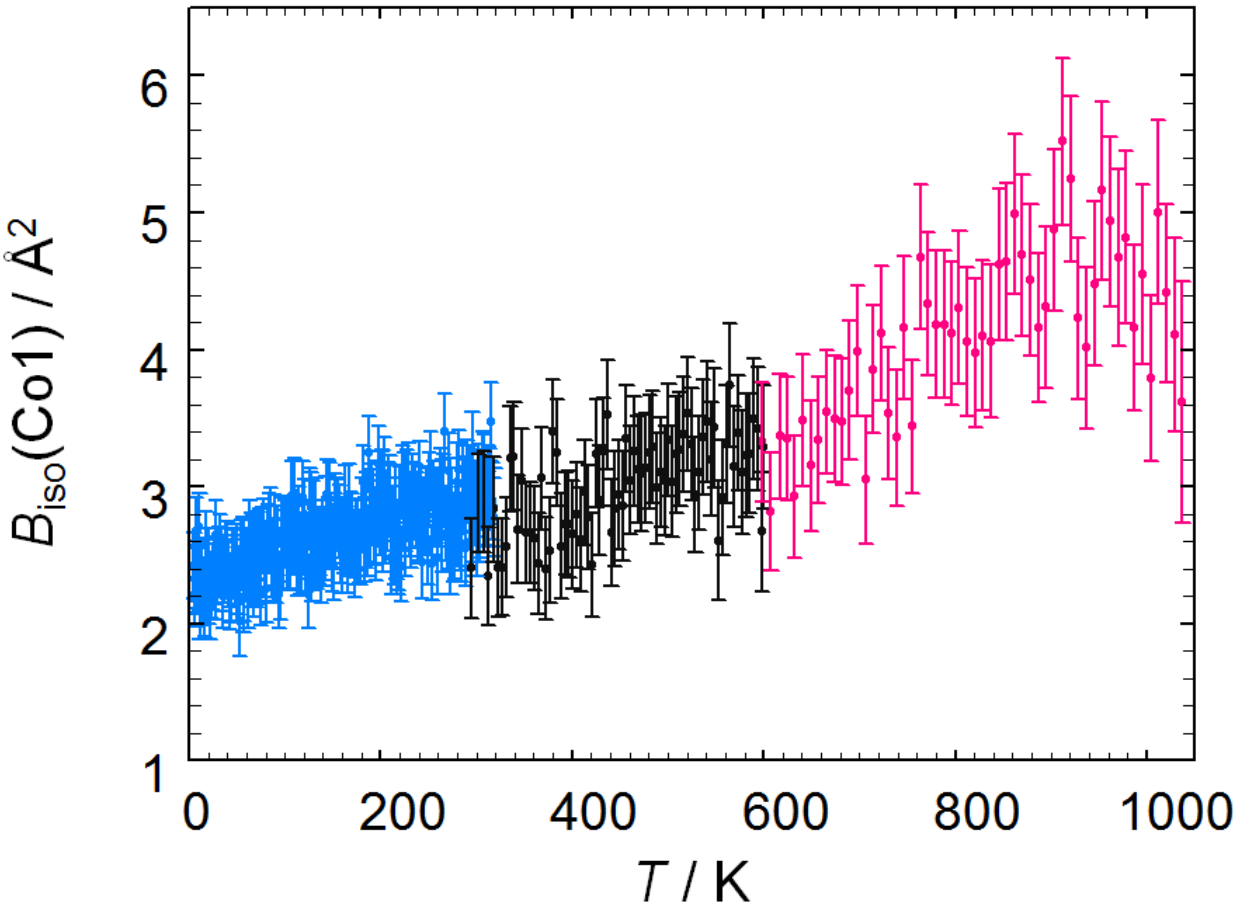

Figure S10: Thermal displacement parameter B_{iso} in Å^2 of Co1 atoms in $^{154}SmCo_5$ as determined by sequential Rietveld refinement based on neutron powder diffraction data (D1B, λ = 2.5218(3) Å) in the temperature range 5.4 K ≤ T ≤ 318.8 K (cryostate, blue symbols), 294.5 K ≤ T ≤ 598.8 K (furnace, fast heating, black symbols) and 607.8 K ≤ T ≤ 1037 K (furnace, slow heating, red symbols). Error bars represent one estimated standard uncertainty ±σ.

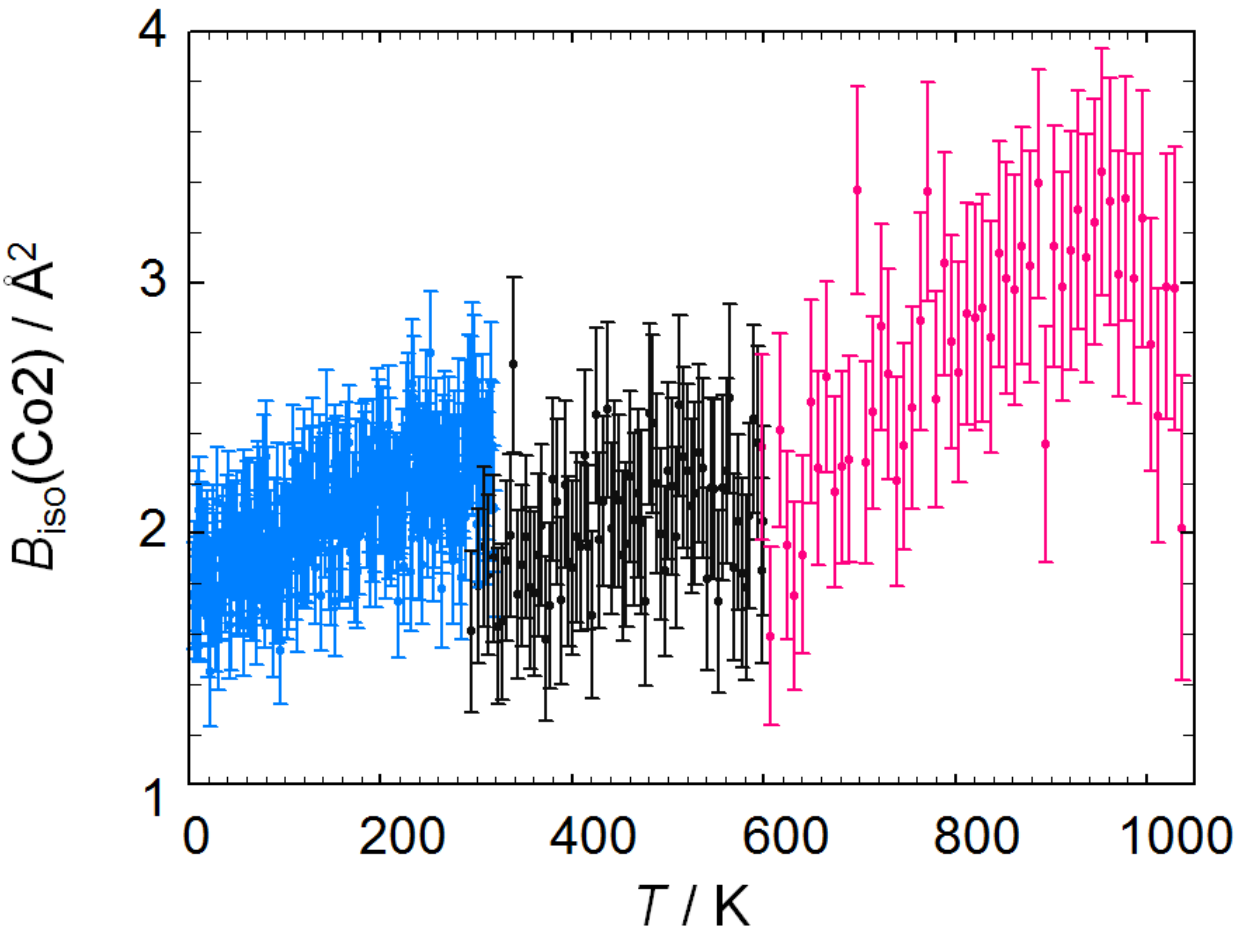

Figure S11: Thermal displacement parameter B_{iso} in Å^2 of Co2 atoms in $^{154}SmCo_5$ as determined by sequential Rietveld refinement based on neutron powder diffraction data (D1B, λ = 2.5218(3) Å) in the temperature range 5.4 K ≤ T ≤ 318.8 K (cryostate, blue symbols), 294.5 K ≤ T ≤ 598.8 K (furnace, fast heating, black symbols) and 607.8 K ≤ T ≤ 1037 K (furnace, slow heating, red symbols). Error bars represent one estimated standard uncertainty ±σ.

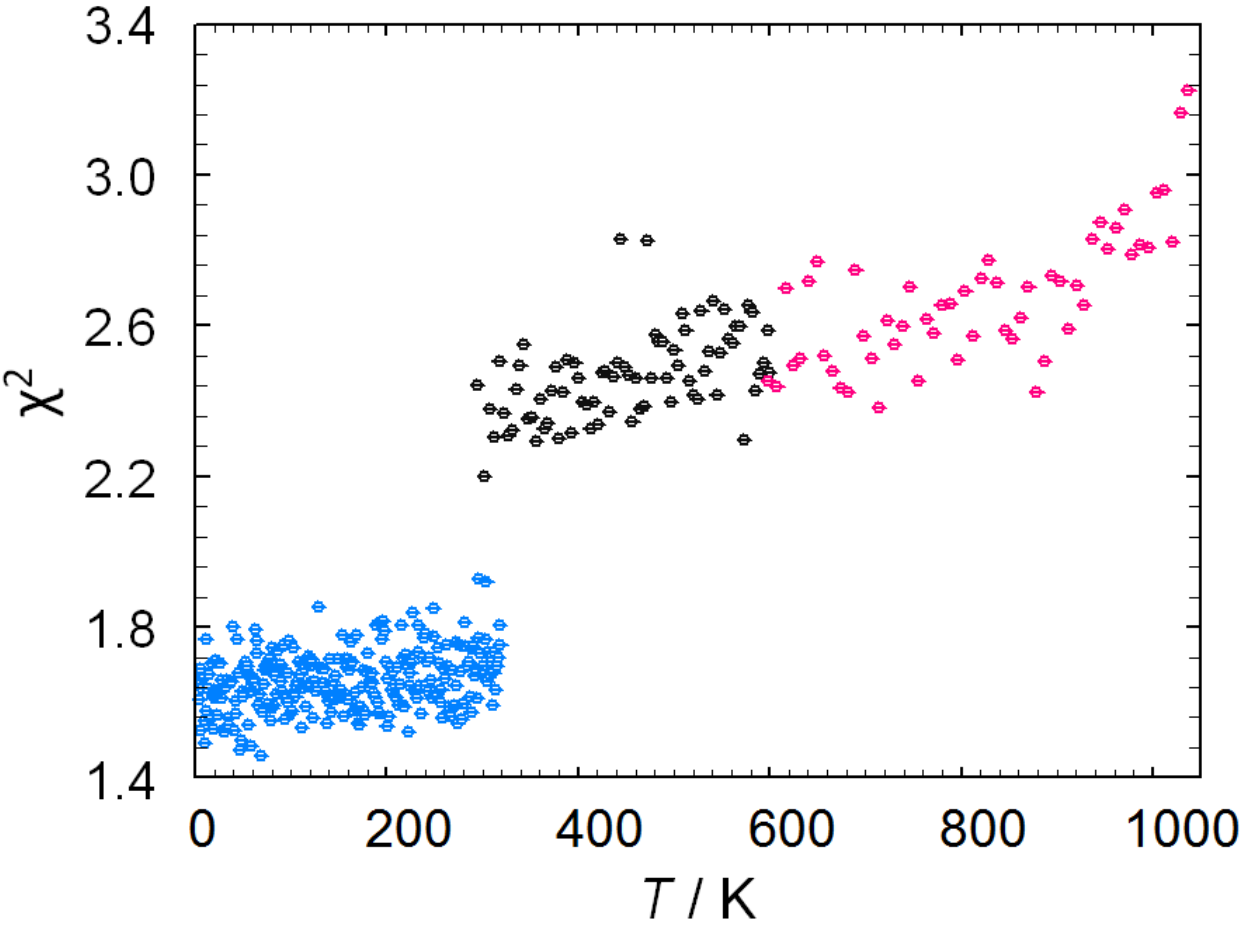

Figure S12: χ^2 for the sequential Rietveld refinement of the crystal and magnetic structure of 154SmCo5 based on neutron powder diffraction data (D1B, λ = 2.5218(3) Å) in the temperature range 5.4 K ≤ T ≤ 318.8 K (cryostate, blue symbols), 294.5 K ≤ T ≤ 598.8 K (furnace, fast heating, black symbols) and 607.8 K ≤ T ≤ 1037 K (furnace, slow heating, red symbols).

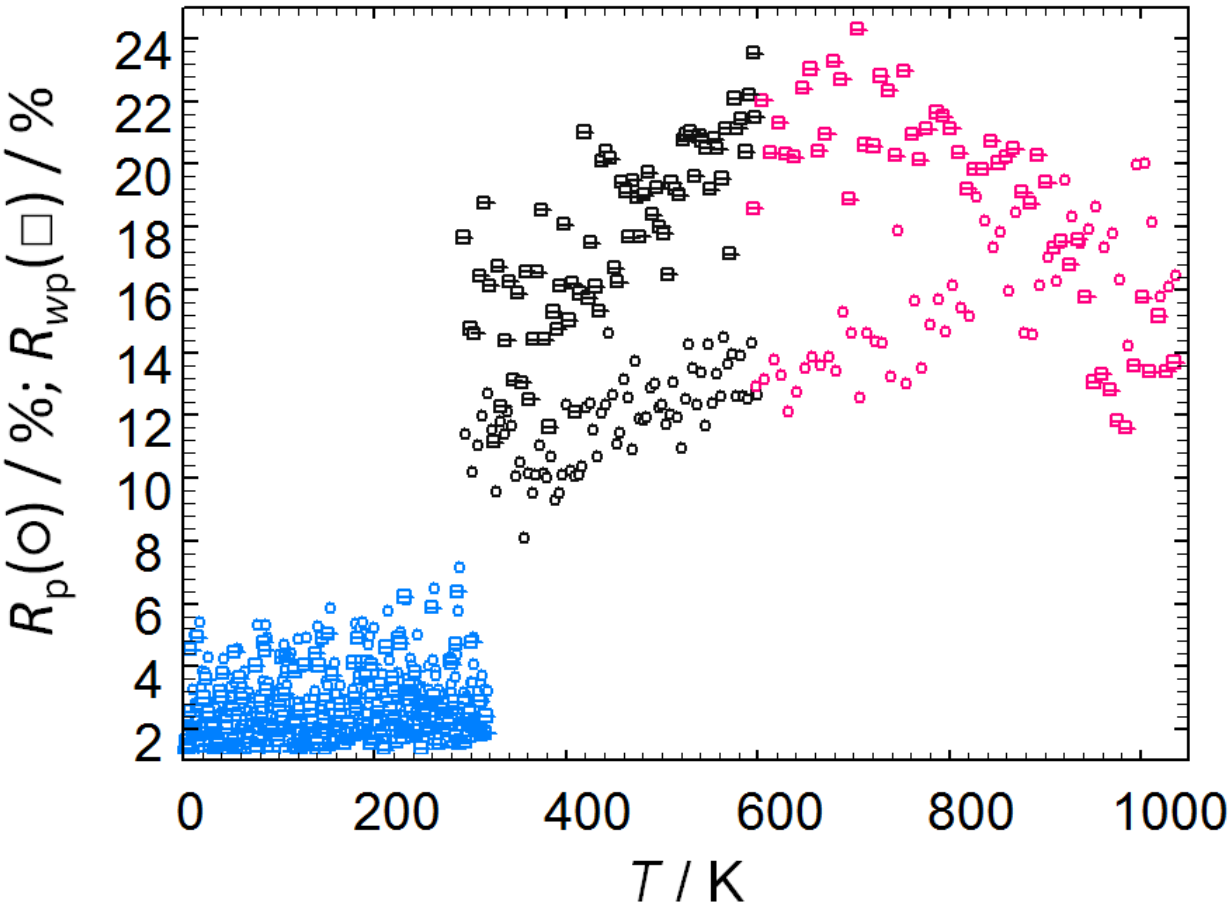

Figure S13: Residual values R_p (circles) and R_{wp} (squares) in % for the sequential Rietveld refinement of the crystal and magnetic structure of $^{154}SmCo_5$ based on neutron powder diffraction data (D1B, λ = 2.5218(3) Å) in the temperature range 5.4 K ≤ T ≤ 318.8 K (cryostate, blue symbols), 294.5 K ≤ T ≤ 598.8 K (furnace, fast heating, black symbols) and 607.8 K ≤ T ≤ 1037 K (furnace, slow heating, red symbols).

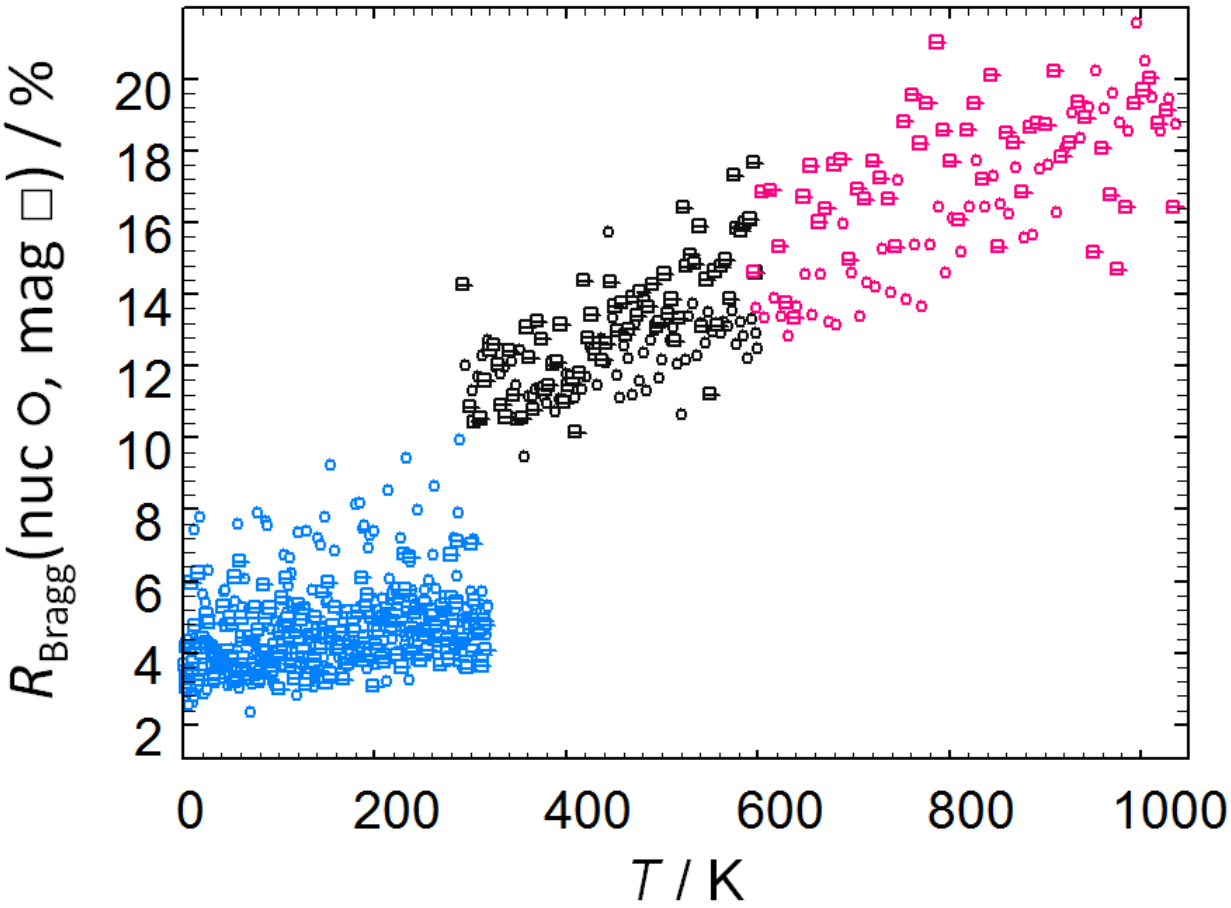

Figure S14: Residual values R_{Bragg} in % for the sequential Rietveld refinement of the crystal (circles) and magnetic (squares) structure of $^{154}SmCo_5$ based on neutron powder diffraction data (D1B, λ = 2.5218(3) Å) in the temperature range 5.4 K ≤ T ≤ 318.8 K (cryostate, blue symbols), 294.5 K ≤ T ≤ 598.8 K (furnace, fast heating, black symbols) and 607.8 K ≤ T ≤ 1037 K (furnace, slow heating, red symbols).

References

[1] Kohlmann, H.; Hein, H.; Kautenburger, R.; Hansen, T. C.; Ritter, C.; Doyle, S. Crystal structure of monoclinic samarium and cubic europium sesquioxides and bound coherent neutron scattering lengths of the isotopes ^{154}Sm and ^{153}Eu. *Z. Kristallogr.* **2016**, *231*, 517-523

[2] Belener, K. L. A.; Kohlmann, H. Reaction pathways of oxide-reduction-diffusion(ORD) synthesis of $SmCo_5$ and *in situ* study of its hydrogen induced amorphization (HIA). *J. Magn. Magn. Mater.* **2014**, *370*, 134-139

[3] Bruker AXS, TOPAS version 5, www.bruker-axs.com

[4] Rodriguez-Carvajal, J. Recent advances in magnetic structure determination neutron powder diffraction. *Z. Phys. B: Condens. Matter* **1993**, *192*, 55-69

[5] Rodriguez-Carvajal, J. FULLPROF version 5.30, Institut Laue-Langevin (ILL), 2012